


Article

# HFCVD Diamond-Coated Mechanical Seals

Raul Simões , Bruno Martins, José Santos and Victor Neto \* 

Centre for Mechanical Technology & Automation (TEMA), Department of Mechanical Engineering, University of Aveiro, 3810-193 Aveiro, Portugal; raul87@ua.pt (R.S.); brunommartins@ua.pt (B.M.); jasantos@ua.pt (J.S.)

\* Correspondence: vneto@ua.pt; Tel.: +351-234-370-200

Received: 31 March 2018; Accepted: 2 May 2018; Published: 3 May 2018



**Abstract:** A mechanical seal promotes the connection between systems or mechanisms, preventing the escape of fluids to the exterior. Nonetheless, due to extreme working conditions, premature failure can occur. Diamond, due to its excellent properties, is heralded as an excellent choice to cover the surface of these devices and extend their lifetime. Therefore, the main objective of this work was to deposit diamond films over mechanical seals and test the coated seals on a water pump, under real working conditions. The coatings were created by hot filament chemical vapor deposition (HFCVD) and two consecutive layers of micro- and nanocrystalline diamond were deposited. One of the main difficulties is the attainment of a good adhesion between the diamond films and the mechanical seal material (WC-Co). Nucleation, deposition conditions, and pre-treatments were studied to enhance the coating. Superficial wear or delamination of the film was investigated using SEM and Raman characterization techniques, in order to draw conclusions about the feasibility of these coatings in the WC-Co mechanical seals with the purpose of increasing their performance and life time. The results obtained gave a good indication about the feasibility of this process and the deposition conditions used, with the mechanical seals showing no wear and no film delamination after a real work environment test.

**Keywords:** mechanical seals; diamond; HFCVD; multi-layer; adhesion; WC-Co; superficial pre-treatments; wear tests

## 1. Introduction

The mechanical seal is a device developed on the late 1930s and the beginning of the 1940s. It allows the connection between systems or mechanisms with the purpose of reducing or eliminating fluid leaking. These components help to prevent the contamination of the surrounding environment and are used on several equipment, such as pumps or turbines, and with different operating fluids [1,2].

There are two types of mechanical seals, minding the existence or not of movement between the moving parts: statics and dynamics. Dynamic seals are the most commonly used, because they ensure a total seal with no leaks and a greater lifetime, with the ability to perform at higher temperatures and pressures [3]. Dynamic seals are composed of a rotating part and a fixed part, and they are used in seals with high requirements, where static seals tend to fail.

The conjugation of friction, high pressures, high temperatures, and the contact with corrosive or toxic fluids lead to the wear of its surface [4–6], causing the failure of these devices. Diamond has proved to be a sublime option as a coating material in this type of application, due to its extreme properties, highlighting its high hardness and low coefficient of friction [7,8].

Nowadays, CVD techniques are the most widely used, enabling the formation of thin diamond films in an easy, cheap manner, and with a satisfactory degree of purity (with properties similar to natural diamond). These methods utilize low pressures and low temperatures, based on the deposition of a chemically-activated gaseous mixture on a substrate, leaving a solid layer on it.

A multilayer film (microcrystalline/nanocrystalline) was adopted in order to retain the best characteristics of each layer, the high fracture strength and good adhesion of microcrystalline diamond (MCD) films, and the low surface roughness of nanocrystalline diamond (NCD) films, ensuring the best performance under demanding tribological applications [9–11].

This work is focused on the utilization of mechanical seals on pumps, specifically on the ones in which water is the working fluid. In this kind of application a reduction of the friction between the pump shaft and seal element is highly appreciated because it can reduce the power loss and the premature shaft wear [3]. It is important to also keep in mind that seal failure is the principle cause of pump malfunction [12]. The paper novelty is, therefore, to evaluate the coating performance in a real water-pumping scenario.

The materials used to make up the sealants are metal alloys, polymers and, especially ceramics. These materials applied to the faces of the seals must have, among other characteristics, low coefficients of friction, high hardness, high corrosion resistance, and high thermal conductivity [5,13]. The most commonly used materials for dynamic seals are: carbon graphite, tungsten carbide (WC), aluminum oxide ( $\text{Al}_2\text{O}_3$ ), and silicon carbide [12,14]. Figure 1 shows an example of a mechanical seal.



**Figure 1.** Example of a mechanical seal.

The main seal comprises two components: a fixed part and a rotating part. The first part is connected to the housing of the machine and remains stable; the rotating part is fixed to the axis of rotation and rotates at the same speed. A secondary seal, which consists on the application of rubber rings on both parts, ensures that there is no leakage between the rotating part and the shaft, as well as between the static part and the housing of the machine (as illustrated on Figure 2) [12]. The material of choice for the secondary seal is usually related with the chemical composition of the working fluid, as well as with the operating temperature [12].

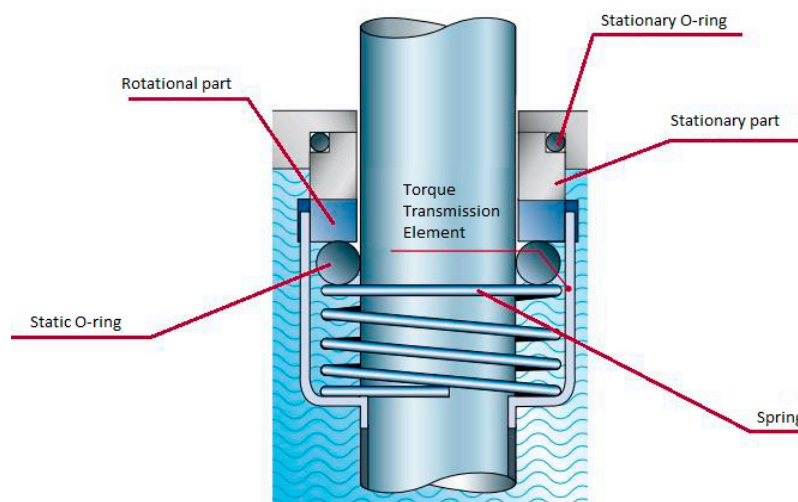


**Figure 2.** Dynamic mechanical seal illustration. Adapted from [12].

There are some goals to achieve, from a tribological point of view, for this study. The first one is the wear and friction reduction, as well as the reduction, or even elimination, of lubrication. These goals must be achieved without any loss of performance. Usually the combination of the friction conditions with the work environment, high pressures, high temperatures, and the possible contact with corrosive fluids lead to surface wear [4–6]. There are four types of surface wear (as illustrated by Figure 3): adhesive wear, abrasive wear, fatigue wear, and corrosive wear [12].



Figure 3. Types of surface wear.

Diamond, with its amazing properties, is an ideal material to significantly improve the mechanical and tribological properties of the seals. The diamond coating ensures a greater reliability, reducing equipment outages (due to faults and maintenance) and operating costs. It could also be used on applications that do not allow the use of lubrication (pharmaceutical products) [5].

Both parts (static and rotating) of the seal can be coated, or just one of them (the other being composed of the original material). If only one of the parts is coated with diamond, the risk of breakage, delamination, and wear rate are reduced (as the deposited surface will slide against a softer material). However, if the goal is to produce a robust and highly-reliable seal, it is recommended to use two rings equally coated with diamond [5].

Currently, there are three sources from which diamond can be obtained: natural deposits, high pressure and high temperature techniques (HPHT), and chemical vapor deposition (CVD) [15]. This last method was the one used in this study, as it uses low pressures and low temperatures. It is based on the deposition of chemically-activated gaseous species on the substrate, leaving thereon a solid layer. The activation of the gaseous mixture can be achieved by hot-filament or microwave plasma [16,17].

The CVD diamond films retain similar properties to natural diamond and, when applied to the face of the seals, can significantly increase their performance and lifetime, desirable characteristics for this type of device [15].

Depending on the size of the deposited grain, the resulting films have their own designation: MCD for crystals sizes between 1–10  $\mu\text{m}$  [6,16,18]; NCD with sizes equal to (or less than 100 nm); and ultrananocrystalline diamond (UNCD) for grain sizes less than 10 nm [6,19]. The MCD film has a higher surface roughness, due to the crystal sizes, resulting in high friction coefficients and wear. MCD films are usually obtained using a mixture of hydrogen ( $\text{H}_2$ ) and oxygen ( $\text{O}_2$ ). Instead, NCD films have a low surface roughness, due to the smaller grains, despite the lower growing rates. These films are possible to obtain, adding Argon (Ar) to the gas mixture previously mentioned.

UNCD films have recently been subject of great study and interest, as they allow for hard, smooth coatings with low deposition temperatures. They do not need any type of surface polishing, being appropriate for tribological applications and showing benefits when applied in mechanical seals [13].

Each type of film has its own particularities and, so, a multilayer coating can be adopted (MCD/NCD), attaining the best of both types and, comparatively with monolayer coatings, are proven to have better adhesion and lower internal tensions [9]. The first deposited layer was an MCD film (with good adhesion and strength) and the second one was an NCD layer (with smaller crystals) to improve the mechanical characteristics of the coating (surface smoothness).

However, in CVD diamond films, there are several aspects that complicate the process, obtaining a suitable adhesion between the film and the substrate is one of the main problems [20]. Factors like: a clean surface; temperature; the chemical nature of the substrate; the nucleation density of the film;

the surface roughness of the substrate; and also the thermal stresses (due to the different coefficients of thermal expansion between diamond and the conventional substrates) can greatly influence the film adhesion [21–23].

Other aspects to take in account are the different parameters to control throughout the deposition process. The pressure inside the chamber is a parameter that can influence the crystal size and growth rate. Liang et al. [24] stated that a pressure below 0.5 kPa leads to smaller crystals and that there is a correlation between pressure and crystal size [24]. Substrate temperature and distance to the filaments also influence the quality of the diamond film obtained, as stated by Song et al. [25], increasing the distance to the filaments leads to a poor quality film.

Another crucial aspect is the gas mixture inside the chamber, for example, Lin et al. [26] concluded that increasing the concentration of Ar in the mixture will increase the growth rate and size of the crystals until a limit of 50%. More than 50% of Ar will decrease those parameters and improve the quality of the film [27].

Several studies can be found on the literature regarding the application of this type of coating on seals with good results. Tomé et al. [28], obtained low friction coefficients (0.05) and no visible wear. Camargo et al. [29] also obtained good results depositing diamond on silicon nitride seals (with a friction coefficient of 0.02), with the capability of working with good stability for thousands of meters. Kovalchenko et al. [30] deposited a diamond coating on a silicon carbide seal and stated that the wear resistance of the device was greatly improved.

## 2. Materials and Methods

The technique used to perform the deposition of the diamond film on the seal was hot-filament chemical vapor deposition (HFCVD). This technique is widely used due to its versatility, simplicity, low cost of implementation, maintenance, and operation, while providing good control of the growth parameters [7,8,31,32].

The surface of four cobalt tungsten carbide (WC-Co) seals will be deposited with diamond film, using the same pre-treatment and deposition conditions. The deposited films will be characterized with SEM imaging and Raman spectroscopy, throughout the processes of treatment and deposition.

The treatment of the substrate samples begins with a gradual polishing; this was accomplished by placing a 15 µm diamond paste on the surface of the seals and applying a relatively constant pressure on these against the rotating plates of the polishing machine (RotoPol-21, Struers A/S, Copenhagen, Denmark). The same method of polishing was then repeated with smaller grain diamond paste (6 µm and 3 µm), followed by ultrasonic cleaning.

The next step is to chemically activate the tungsten carbide grains and remove the cobalt concentration from the surface of the seals. This chemical attack was performed in two distinct stages: the first step is to place the samples on a solution called “Murakami” (10 g  $K_3(Fe(CN)_6)$  + 10 g KOH + 100 mL  $H_2O$ ) for 6 min, in an ultrasonic bath at room temperature; the second step is to remove the cobalt from the surface of the seal, using a solution of nitric acid (1 mL 46 wt %  $HNO_3$  + 9 mL 30% *m/v*  $H_2O_2$ ) for 10 s [20,33,34]. The samples were cleaned in an ultrasonic bath in distilled water for 15 min, between and at the end of both steps.

To improve diamond nucleation, ensuring better homogeneity of the films and good adhesion levels, a final pretreatment was performed on the surface of the seals. The substrate was ultrasonically cleaned in an ethanol bath for 15 min, followed by an abrasion of the substrate surface with diamond powder on the plates of the same polishing machine (similarly to the polishing step), for 25 min with diamond particles of 3 µm (DP-Paste M, Struers A/S, Copenhagen, Denmark). This process will increase the roughness of the substrate surface and, hence, increase the specific surface to be coated, which optimizes adhesion. This step concludes the preparation process of the four samples to be deposited.

The surface roughness of the samples was measured using a Hommel Tester T1000 (JENOPTIK AG, Jena, Germany) before the deposition of the diamond film to compare with the results obtained

after the CVD deposition. Table 1 summarizes the conditions used in the process regarding the four samples.

**Table 1.** CVD deposition conditions.

Parameters	Samples 1 and 2		Samples 3 and 4	
	1st Deposition Microcrystalline Layer	2nd Deposition Nanocrystalline Layer	1st Deposition Microcrystalline Layer	2nd Deposition Nanocrystalline Layer
Gas flow (sccm)	200	200	200	200
CH <sub>4</sub> (sccm)	2	2	2	2
H <sub>2</sub> (sccm)	198	34	198	34
Ar (sccm)	0	164	0	164
Filament/Substrate distance (mm)	8	8	8	8
Power intensity (VxA)	24 × 43	22 × 35	30 × 32	25 × 33
Pressure (Torr)	30	30	30	30
Deposition time (h)	3	5	3	5
Substrate temperature (°C)	500	375	450	375

For both depositions, five tantalum filaments (0.02 mm diameter) were arranged in a horizontal plane, with about 100 nm long. The filament spacing was 10 mm, they were cleaned with acetone and positioned 8 mm from the face of the samples to be coated. The substrate temperature was measured with the help of a thermocouple placed close to the samples. The growth was carried out at a constant pressure of 30 Torr and with a total gas flow of 200 sccm. The main differences between the two depositions are the gas mixture composition (the addition of Ar allowed the growth of smaller crystals (NCD)), and the deposition time (the presence of Ar also reduce the growth rate).

### 3. Results

#### 3.1. Seal Characterization

##### 3.1.1. Roughness Measurements

After the deposition process, the surface roughness of the samples was once again measured and Tables 2 and 3 summarize the measurements before and after deposition. Samples 3 and 4 were not measured at the beginning.

It is possible to observe a decrease in the total surface roughness values of the seals. As for the values of the average roughness, these were similar to the previously-obtained values, although a brief decrease of this value on a surface deposited with nanocrystalline diamond could be expected.

**Table 2.** Surface roughness before deposition.

Roughness Parameter	Sample 1	Sample 2
$R_a$ ( $\mu\text{m}$ )	0.075	0.093
$R_t$ ( $\mu\text{m}$ )	0.916	0.910

**Table 3.** Surface roughness after deposition.

Roughness Parameter	Sample 1	Sample 2	Sample 3	Sample 4
$R_a$ ( $\mu\text{m}$ )	0.077	0.072	0.078	0.077
$R_t$ ( $\mu\text{m}$ )	0.19	0.17	0.2	0.17

##### 3.1.2. SEM Imaging

SEM images of the samples after the first deposition are presented in Figure 4, where it is possible to observe the existence of a few disordered diamond crystals.



In Figure 5 four SEM images are presented (with two different magnifications) from the surface of the seals after the second deposition. With a superior magnification of the surfaces, the presence of well-defined diamond grains of reduced size is more evident. This thin film of NCD filled the gaps that existed on the MCD film, resulting in a smoother surface. Observing these images, it is possible to estimate the approximate size of the diamond crystals. On average, “balls” with approximate  $3\ \mu\text{m}$  are noticed, with each “speck” inside it (diamond grains) being about  $100\ \text{nm}$  (NCD film deposited on the surface of the seals).

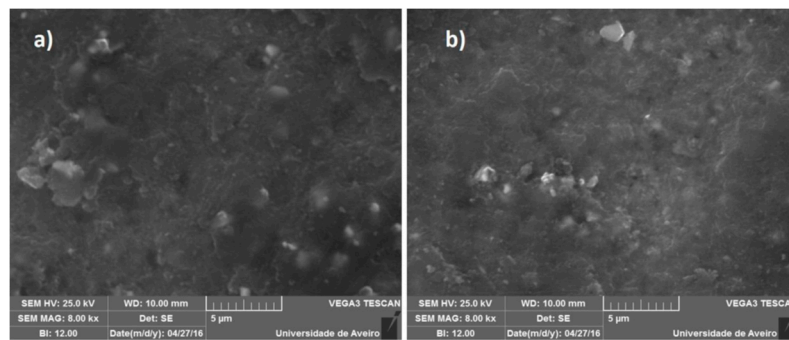


**Figure 4.** SEM images after first deposition: (a) Sample 1,  $8000\times$  and (b) Sample 2,  $8000\times$ .

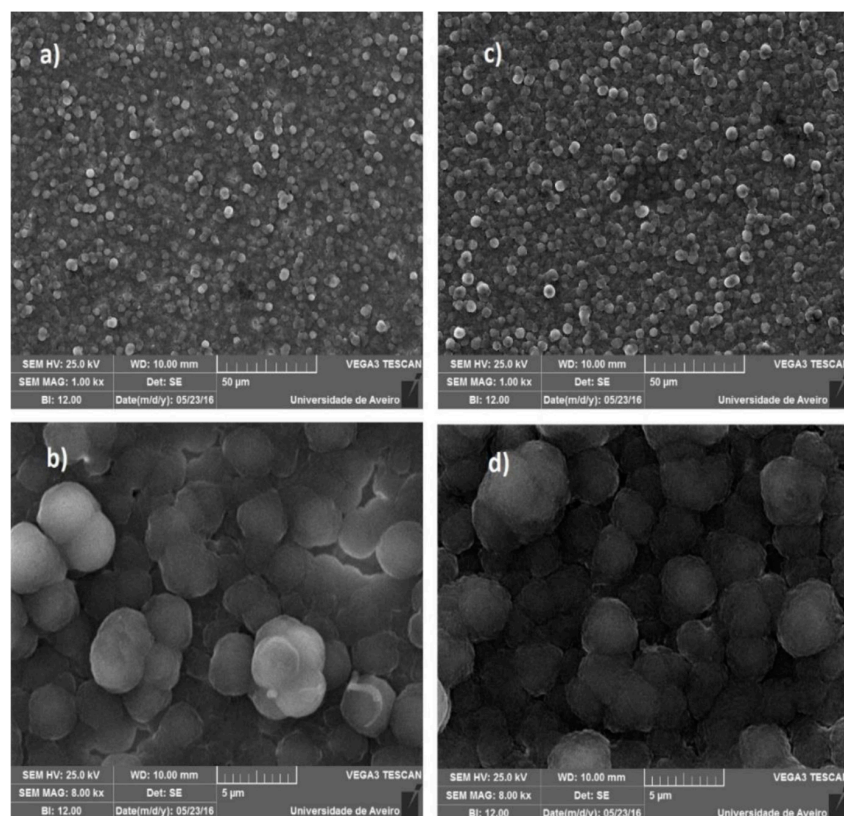


**Figure 5.** SEM images—second deposition: (a) Sample 3,  $1000\times$ ; (b) Sample 3,  $8000\times$ ; (c) Sample 4,  $1000\times$ ; and (d) Sample 4,  $8000\times$ .

In Figure 6 one can observe the differences between the film formed in the inner edge and upper edge of the seal. The presence of diamond grains on both edges of the seals is observed, presenting a closed film.

Finally, Figure 7 is a SEM image of the inner edge of the coated seals after the second deposition (2000× for the Sample 3 and 8000× for the Sample 4). It is possible to observe a good-quality closed film with small, well-defined diamond crystals.

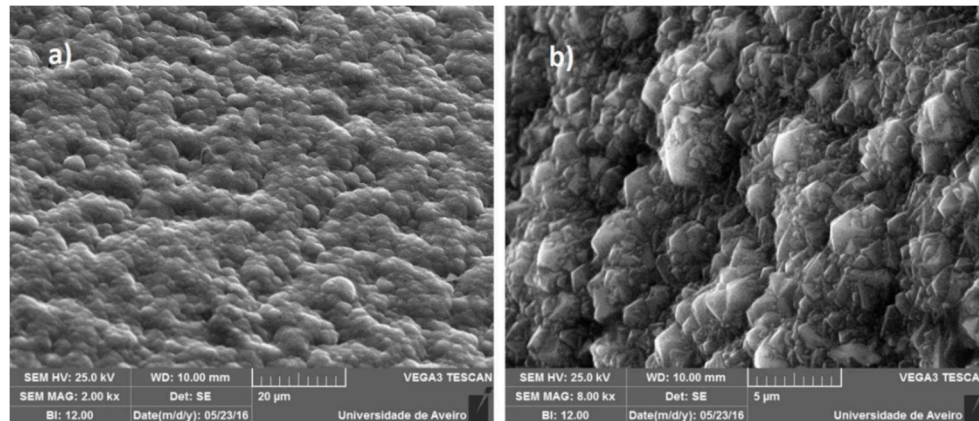


Figure 6. SEM image—second deposition inner edge: (a) Sample 3, 2000× and (b) Sample 4, 8000×.

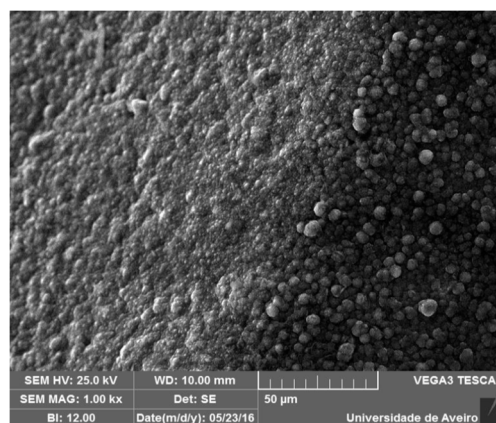


Figure 7. SEM image of Sample 4—second deposition—inner edge/upper edge transition.

### 3.1.3. Raman Spectroscopy

Following this evaluation with the help of the SEM images, the samples were examined by Raman spectroscopy. From Figure 8 it is possible to evaluate the quality of the film and the amount of  $sp^3$  diamond present in the sample compared to the other disordered carbon phases also present.

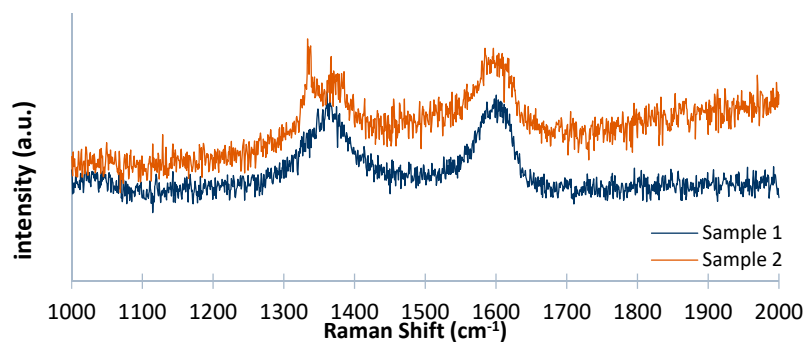


Figure 8. Raman spectra from the first deposition.

The samples exhibit a peak at  $1335\text{ cm}^{-1}$ , the characteristic peak of diamond (may vary between  $1331$  and  $1336\text{ cm}^{-1}$ ), especially Sample 2 with a strong and narrow peak. This is an important aspect, since in NCD films the characteristic peak of diamond decreases when compared to the same one observed in MCD films, increasing in intensity the peak assigned to the D band of graphite.

It is noticeable that a wide peak centered at approximately  $1600\text{ cm}^{-1}$  is associated with the  $sp^2$  carbon, which is related to the decrease in grain size, where the peak assigned to the G band ( $1580\text{ cm}^{-1}$ ) shifts to about  $1600\text{ cm}^{-1}$ . This is another indication of the presence of a film with a small grain size [24,26,35–38].

Analyzing with Raman the silicon sample (deposited at the same time), a small peak at approximately  $1332\text{ cm}^{-1}$  is noticeable (Figure 9). This is due to the presence of Ar in the gas mixture, which makes possible the presence of smaller grains. By comparing this result with the result from Figure 8, it is possible to examine a more linear spectrum, with the different well-defined peaks, in accordance with those defined in the literature for NCD depositions. This confirms that silicon is a more favorable material for diamond growth compared to WC-Co.

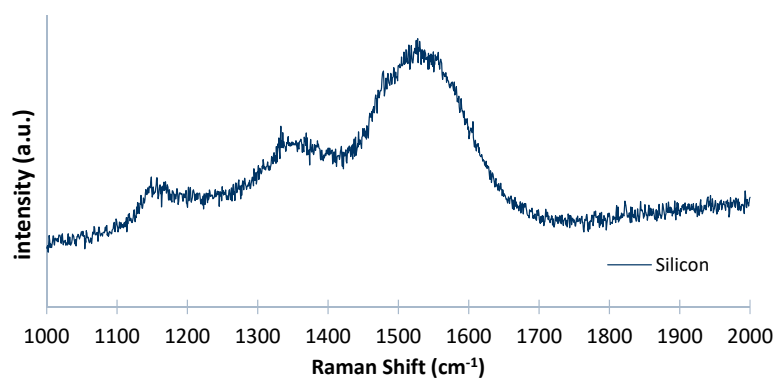


Figure 9. Silicon Raman spectra from first deposition.

Regarding the samples from the second deposition, a well-defined peak at  $1334\text{ cm}^{-1}$  is noticeable, as shown in Figure 10, but exhibiting a lower intensity compared to the peak shown in the MCD films. As stated before, this was expected, as the introduction of Ar in the gas mixture reduces the intensity of the characteristic peak. Additionally, the presence of peaks around  $1150\text{ cm}^{-1}$  and  $1480\text{ cm}^{-1}$  is a good indicator of the non-diamond carbon structures (graphite and diamond-like-carbon (DLC)) present in the film. Furthermore, the spectrum is completed with a peak at approximately  $1512\text{ cm}^{-1}$  with a large width at half height, associated with  $sp^2$  carbon (amorphous carbon  $\approx 1500\text{ cm}^{-1}$ ) [24,26,35,36,38].

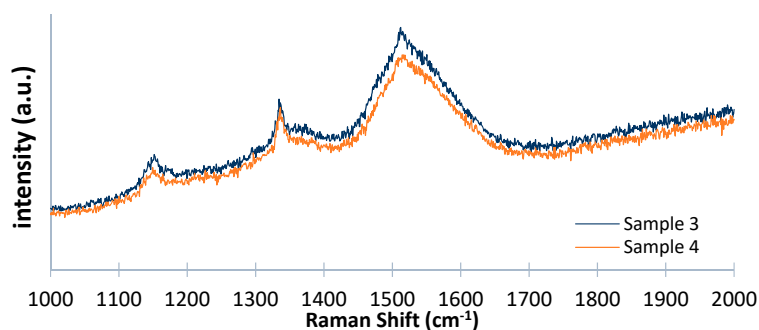


Figure 10. Raman spectra from the second deposition.

This (Figure 10) was the best result obtained, very similar to the results presented in the available literature. Consequently, the samples from the second deposition will be used on the water pump to perform the wear tests.



### 3.1.4. Mass Measurements

Before the wear tests, the mass of the samples were measured to further evaluate the possible mass loss after the seals performed on the water pump. The mass values obtained are shown in Table 4.

**Table 4.** Seal mass after deposition.

Parameter	Sample 1	Sample 2	Sample 3	Sample 4
Mass (g)	37.853	37.891	37.992	37.872

### 3.2. Wear Tests and Characterization

After the wear tests were carried out, the seals were examined using SEM and Raman analysis, to compare the results obtained with the ones performed before the seals were subjected to their natural working environment. The test was performed in an Ebara Pump AGA 1.50 M (EBARA Pumps Europe S.p.A., Trento, Italy), generally used in domestic environments, for example, car washes or small gardens.

In Figure 11 [39] one can observe the technical design of the mechanical seal on the pump. The deposited seals were cleaned again, before being installed, in an ultrasonic bath for 15 min to remove any residues present on their surface that could interfere with their performance.

The pump was used to suck water from a well for irrigation, with a working temperature of about 20 °C at atmospheric pressure, for a period of 5 h. The rotation speed was about 3000 rpm, which can be translated to a distance (travelled by the seal) of about 86 km. Table 5 summarizes the working parameters used on this experimental setup.

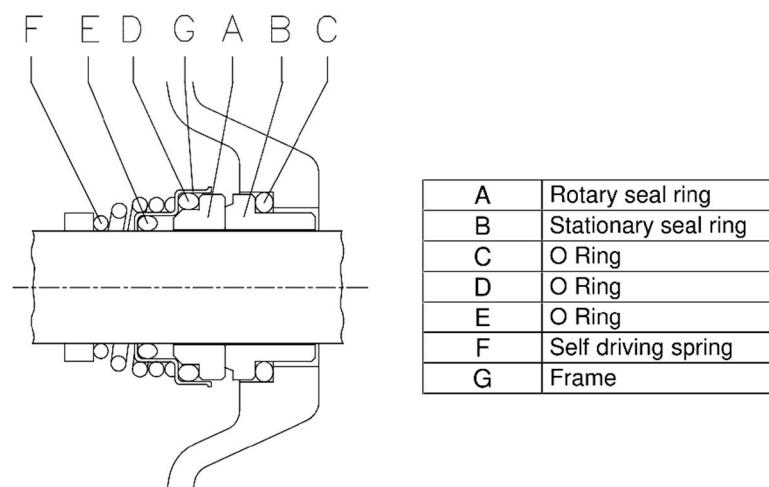


**Figure 11.** Technical design of the used mechanical seal (EBARA).

**Table 5.** Parameters of the wear tests of the seals on the water pump.

Parameter	Value
Work fluid	Water
Work temperature	20 °C
Work pressure	1 atm
Rotational speed	3000 rpm
Working time	5 h
Sliding distance of the seals	86 km

After the wear tests the mechanical seals were analyzed using SEM imaging, Raman analysis, and by measuring its mass. If the film is still present and in good condition, it is possible to state that the experimental procedure was well performed, and the adhesion and film quality are suitable for this type of application. The seals were cleaned once again in an ultrasonic bath for 15 min and the samples were named as: Sample 3 static seal and Sample 4 rotational seal.

### 3.2.1. SEM Analysis

Analyzing Figure 12, in comparison with Figure 4a,b, it is possible to notice that there is no evidence of film delamination. The film remains homogeneous and with good quality. The nanocrystalline diamond deposited in the second layer favorably resisted contact between the rings and that the microcrystalline layer deposited first was very important for a good adhesion.

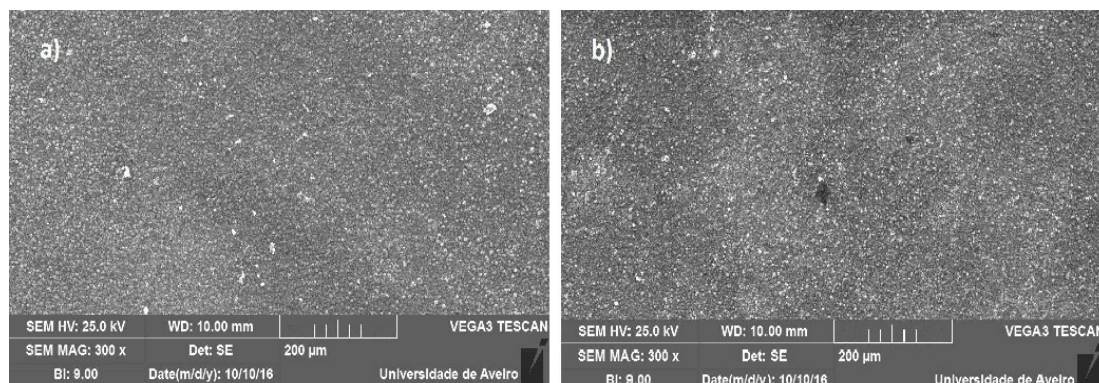


**Figure 12.** Seal SEM image after service: (a) rotational seal 300× and (b) static seal 300×.

Figure 13 illustrates the SEM image of the inside of the seal, proving that no delamination of the coating occurred, exhibiting an enclosed film with well-defined and small crystals without any type of wear.

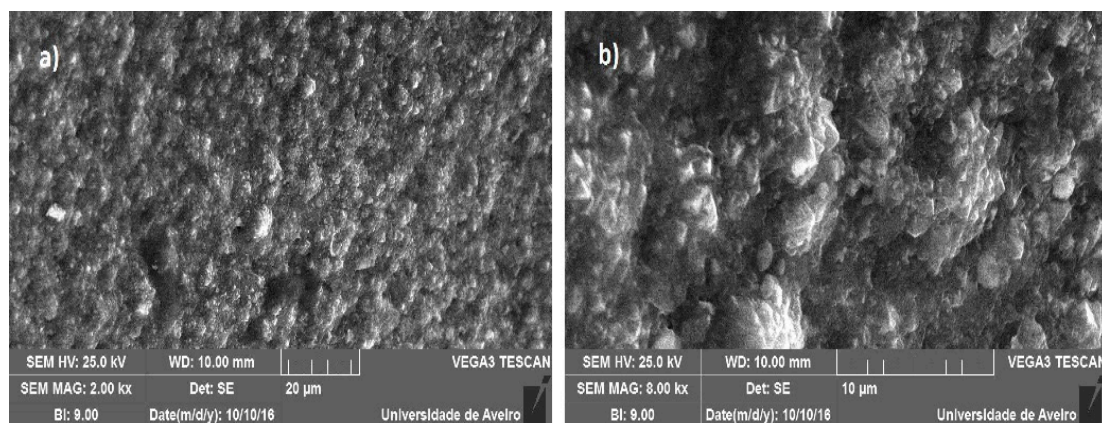


**Figure 13.** Seal SEM image after service—inner edge: (a) rotational seal 2000× and (b) static seal 8000×.

### 3.2.2. Raman Spectroscopy

Analyzing Figure 14, a peak is evident at  $1335\text{ cm}^{-1}$ , attributed to diamond, and one at  $1500\text{ cm}^{-1}$ , associated with the amorphous carbon. A peak around  $1140\text{ cm}^{-1}$  is also visible, generally attributed in the literature to the presence of an NCD film.

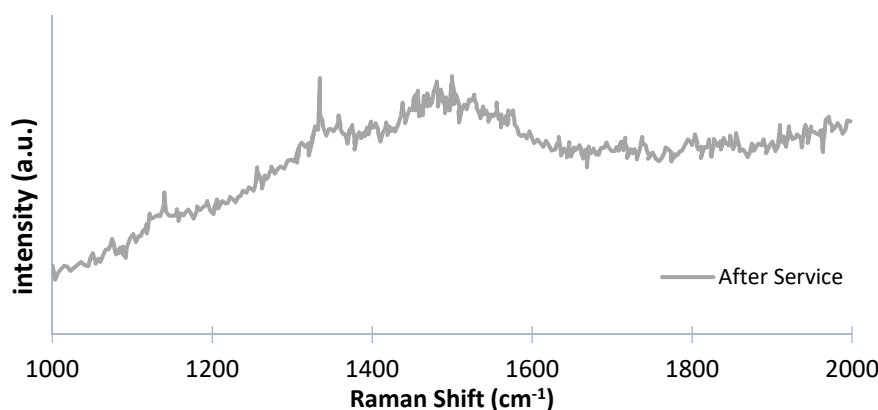


Figure 14. Raman of the seals after wear tests.

### 3.2.3. Seal Mass after Pump Wear Tests

Table 6 resumes the measurements before and after the wear tests are performed, allowing the evaluation of the quantity of the film lost.

Table 6. Seals' mass after working on the pump.

Sample	Before Test	After Test	Loss of Material
Sample 3 (static)	37.992 g	37.921 g	0.001 g
Sample 4 (dynamic)	37.872 g	37.869 g	0.003 g

By making a comparison with the mass of the seals before the wear tests were carried out on the pump, a minimum difference is verified, which shows that the film delamination did not occur on the packing surface and that the surface wear was practically non-existent.

It can be considered that the different pre-treatments and deposition conditions, which have a direct influence on the quality and adhesion of the film, were well employed. The use of multilayers allowed a good adhesion of the film, and the deposited NCD top layer provided a good performance of the seals.

## 4. Conclusions

This work consisted of a multilayered deposition of thin films on WC-Co mechanical seals by the HFCVD technique. These were installed in a pump and worked in the suction of water from a well for irrigation for 5 h, which corresponds to a working distance of about 86 km.

The main objectives were to evaluate the deposited film, its morphology, quality, grain size, and surface wear of the seals after working in the pump.

The obtained images revealed the presence of a homogeneous, coalescing film of good quality, with well-defined diamond grains (of small size) of about 100 nm, proving the presence of an NCD film in the most superficial layer of the sample.

After the verification of the existence of a quality diamond film, the seals were subjected to the wear tests to verify their behavior, verifying that no type of failure or leakage of fluid occurred, and it can be concluded that these showed good performance.

The mass of the seals was measured, and this measurement was also carried out after the wear tests, with an insignificant difference between the values of both measurements, which corroborates with the conclusions drawn from the previously-used techniques.

The deposition conditions employed were effective for the deposition of multilayer diamond films on this type of substrate. The use of this type of coating proved to be useful and allowed the retention of the best characteristics of each type of layer, being a perspicacious method to improve

adhesion, but, at the same time, to provide a smooth surface (with reduced roughness), an important characteristic for optimizing the performance of the seals.

**Author Contributions:** R.S. has analyzed the results and wrote the paper; B.M. performed most of the experiments presented here; J.S. helped in conceiving and designing the experiments and performed some of the experiments; and V.N. conceived and designed the experiments, analyzed the results, and wrote the paper.

**Funding:** This work was supported by TEMA under the project UID/EMS/00481/2013 and project CENTRO-01-0145-FEDER-022083, financed by FCT/MEC through national funds and the co-funding of FEDER, within the PT2020 Partnership Agreement and Compete 2020.

**Conflicts of Interest:** The authors declare no conflict of interest.

## References

- Kelly, P.J.; Arnell, R.D.; Hudson, M.D.; Wilson, A.E.J.; Jones, G. Enhanced mechanical seal performance through CVD diamond films. *Vacuum* **2001**, *61*, 61–74. [CrossRef]
- Santos, J.A.; Ruch, V.F.; Grácio, J. Mechanical properties of nanocrystalline diamond coating on WC substrate with different interlayers. In Proceedings of the NANOSMAT 5th International Conference on Surface, Coatings and Nanostructured Materials, Reims, France, 19–21 October 2010.
- Rodrigues, A.J. Estudo de Causas de Falhas em Selos Mecânicos de Bombas Centrífugas Para Circulação de Óleo Térmico; Master's Thesis, Universidade Estadual Paulista Júlio de Mesquita Filho, Guaratinguetá, Brazil, February 2012.
- Jones, G.A. On the tribological behaviour of mechanical seal face materials in dry line contact: Part II. Bulk ceramics, diamond and diamond-like carbon films. *Wear* **2004**, *256*, 433–455. [CrossRef]
- Hollman, P.; Björkman, H.; Alahelisten, A.; Hogmark, S. Diamond coatings applied to mechanical face seals. *Surf. Coat. Technol.* **1998**, *105*, 169–174. [CrossRef]
- Santos, J.A.; Neto, V.F.; Ruch, D.; Grácio, J. Nanocrystalline diamond coatings for mechanical seals applications. *J. Nanosci. Nanotechnol.* **2012**, *12*, 6835–6839. [CrossRef] [PubMed]
- May, P.W. Diamond thin films: A 21st-century material. *Philos. Trans. R. Soc. A Math. Phys. Eng. Sci.* **2000**, *358*, 473–495. [CrossRef]
- Lee, S.-T.; Lin, Z.; Jiang, X. CVD diamond films: Nucleation and growth. *Mater. Sci. Eng. R Rep.* **1999**, *25*, 123–154. [CrossRef]
- Chen, N.; Pu, L.; Sun, F.; He, P.; Zhu, Q.; Ren, J. Tribological behavior of HFCVD multilayer diamond film on silicon carbide. *Surf. Coat. Technol.* **2015**, *272*, 66–71. [CrossRef]
- Chen, N.C.; Sun, F.H. Friction and wear performances of hot filament chemical vapor deposition multilayer diamond films coated on silicon carbide under water lubrication. *J. Shanghai Jiaotong Univ.* **2013**, *18*, 237–242. [CrossRef]
- Luo, J.-L.; Ying, X.-T.; Wang, P.-N.; Chen, L.-Y. Growth and optical properties of nanocrystalline/microcrystalline diamond multilayer films. *J. Korean Phys. Soc.* **2005**, *46*, 224–228.
- GRUNDFOS Management A/S. *Mechanical Shaft Seals for Pumps*, 1st ed.; GRUNDFOS Management A/S: Bjerringbro, Denmark, 2009.
- West, C.; Netzel, J. Diamond—Its effect on the seal industry. *World Pumps* **2008**, *2008*, 50–52. [CrossRef]
- Ekk Technologies Mechanical Seals. Available online: <https://www.ekkeagle.com/en/technology/mechanical/> (accessed on 9 March 2018).
- Spitsyn, B.V.; Bouilov, L.L.; Alexenko, A.E. Origin, state of the art and some prospects of the diamond CVD. *Braz. J. Phys.* **2000**, *30*, 471–481. [CrossRef]
- Tjong, S.C.; Chen, H. Nanocrystalline materials and coatings. *Mater. Sci. Eng. R Rep.* **2004**, *45*, 1–88. [CrossRef]
- Matsumoto, S.; Sato, Y.; Kamo, M.; Setaka, N. Vapor deposition of diamond particles from methane. *Jpn. J. Appl. Phys.* **1982**, *21*, L183–L185. [CrossRef]
- Gruen, D.M. Nanocrystalline diamond films. *Annu. Rev. Mater. Sci.* **1999**, *29*, 211–259. [CrossRef]
- Krauss, A.R.; Auciello, O.; Gruen, D.M.; Jayatissa, A.; Sumant, A.; Tucek, J.; Mancini, D.C.; Moldovan, N.; Erdemir, A.; Ersoy, D.; et al. Ultrananocrystalline diamond thin films for MEMS and moving mechanical assembly devices. *Diam. Relat. Mater.* **2001**, *10*, 1952–1961. [CrossRef]



20. Cabral, G.; Madaleno, J.C.; Titus, E.; Ali, N.; Grácio, J. Diamond chemical vapour deposition on seeded cemented tungsten carbide substrates. *Thin Solid Films* **2006**, *515*, 158–163. [[CrossRef](#)]
21. Silva, V.A.; Fernandes, A.J.; Costa, F.M.; Silva, R. Deposição direta de diamante CVD em compósitos cerâmicos Si<sub>3</sub>N<sub>4</sub>/SiC. *Rev. Bras. Apl. Vácuo* **2000**, *19*, 27–32.
22. Fujiy, O.K.; Trava-Airoldi, V.J.; Corat, E.J.; Ferreira, M.J.; Amorim, A.; Moro, J.R. Growth rate of the CVD diamond films on molybdenum surfaces. Taxa de crescimento de filmes de diamante CVD em superfícies de molibdênio. *Rev. Esc. Minas* **2007**, *60*, 227–231. [[CrossRef](#)]
23. Nakamura, Y.; Sakagami, S.; Amamoto, Y.; Watanabe, Y. Measurement of internal stresses in CVD diamond films. *Thin Solid Films* **1997**, *308*, 249–253. [[CrossRef](#)]
24. Liang, X.; Wang, L.; Zhu, H.; Yang, D. Effect of pressure on nanocrystalline diamond films deposition by hot filament CVD technique from CH<sub>4</sub>/H<sub>2</sub> gas mixture. *Surf. Coat. Technol.* **2007**, *202*, 261–267. [[CrossRef](#)]
25. Song, G.H.; Yoon, J.H.; Kim, H.S.; Sun, C.; Huang, R.F.; Wen, L.S. Influence of hot filaments arranging on substrate temperature during HFCVD of diamond films. *Mater. Lett.* **2002**, *56*, 832–837. [[CrossRef](#)]
26. Lin, T.; Yu, G.Y.; Wee, A.T.S.; Shen, Z.X. Compositional mapping of the argon-methane-hydrogen system for polycrystalline to nanocrystalline diamond film growth in a hot-filament chemical vapor deposition system. *Appl. Phys. Lett.* **2000**, *77*, 2692–2694. [[CrossRef](#)]
27. Zhang, Y.F.; Zhang, F.; Gao, Q.J.; Yu, D.P.; Peng, X.F.; Lin, X.D. Synthesis of nano-crystalline diamond film in hot filament chemical vapour deposition by adding Ar. *Chin. Phys. Lett.* **2001**, *18*, 286–288. [[CrossRef](#)]
28. Tomé, M.A.; Fernandes, A.J.S.; Oliveira, F.J.; Silva, R.F.; Carrapichano, J.M. High performance sealing with CVD diamond self-mated rings. *Diam. Relat. Mater.* **2005**, *14*, 617–621. [[CrossRef](#)]
29. Camargo, S.S.; Gomes, J.R.; Carrapichano, J.M.; Silva, R.F.; Achete, C.A. Silicon-incorporated diamond-like coatings for Si<sub>3</sub>N<sub>4</sub> mechanical seals. *Thin Solid Films* **2005**, *482*, 221–225. [[CrossRef](#)]
30. Kovalchenko, A.M.; Elam, J.W.; Erdemir, A.; Carlisle, J.A.; Auciello, O.; Libera, J.A.; Pellin, M.J.; Gruen, D.M.; Hryn, J.N. Development of ultrananocrystalline diamond (UNCD) coatings for multipurpose mechanical pump seals. *Wear* **2011**, *270*, 325–331. [[CrossRef](#)]
31. Moro, J.R.; Nascente, P.A.P.; Trava-Airoldi, V.J.; Corat, E.J.; Alves, A.R.; Alves, A. Crescimentos sucessivos de filmes de diamante cvd em grandes áreas. *Rev. Bras. Apl. Vácuo* **2007**, *26*, 83–87.
32. Liu, H.; Dandy, D.S. Diamond chemical vapor deposition: Nucleation and early growth stages. In *Diamond Chemical Vapor Deposition*; Noyes Publication: Saddle River, NJ, USA, 1995; pp. 46–126. ISBN 9780815513803.
33. Cabral, E.G.S.S. Development and Application of Diamond Coatings onto Cutting Tools to Machine EDM Electrodes for Mould Industry. Ph.D. Thesis, University of Aveiro, Aveiro, Portugal, December 2006.
34. Polini, R.; Delogu, M.; Marcheselli, G. Adherent diamond coatings on cemented tungsten carbide substrates with new Fe/Ni/Co binder phase. *Thin Solid Films* **2006**, *494*, 133–140. [[CrossRef](#)]
35. Feng, J.; Li, S.; Luo, H.; Wei, Q.; Wang, B.; Li, J.; Hu, D.; Mei, J.; Yu, Z. Preparation and characterization of ultrananocrystalline diamond films in H<sub>2</sub>/Ar/CH<sub>4</sub> gas mixtures system with novel filament structure. *J. Cent. South Univ.* **2015**, *22*, 4097–4104. [[CrossRef](#)]
36. Kuzmany, H.; Pfeiffer, R.; Salk, N.; Günther, B. The mystery of the 1140 cm<sup>-1</sup> Raman line in nanocrystalline diamond films. *Carbon* **2004**, *42*, 911–917. [[CrossRef](#)]
37. Kromka, A.; Breza, J.; Kadlečíková, M.; Janík, J.; Balon, F. Identification of carbon phases and analysis of diamond/substrate interfaces by Raman spectroscopy. *Carbon* **2005**, *43*, 425–429. [[CrossRef](#)]
38. Cebik, J.; McDonough, J.K.; Peerally, F.; Medrano, R.; Neitzel, I.; Gogotsi, Y.; Osswald, S. Raman spectroscopy study of the nanodiamond-to-carbon onion transformation. *Nanotechnology* **2013**, *24*, 205703. [[CrossRef](#)] [[PubMed](#)]
39. Donnet, C.; Erdemir, A. *Tribology of Diamond-Like Carbon Films*; Springer: Berlin, Germany, 2008; ISBN 978-0-387-30264-5.

